IDENTIFICATION OF OBJECTS IN AN ACOUSTIC WAVEGUIDE:

NUMERICAL RESULTS AND AN INTRODUCTION TO AN ALTERNATE APPROACH VIA THE METHOD OF IMAGES

by

Lawrence C. Udeigwe

A thesis submitted to the Faculty of the University of Delaware in partial fulfillment of the requirements for the degree of Master of Science in Applied Mathematics

Summer 2006

IDENTIFICATION OF OBJECTS IN AN ACOUSTIC WAVEGUIDE:

NUMERICAL RESULTS AND AN INTRODUCTION TO AN ALTERNATE APPROACH VIA THE METHOD OF IMAGES

by

Lawrence C. Udeigwe

Approved: _____

Robert P. Gilbert, Ph.D.
Professor in charge of thesis on behalf of the Advisory Committee

Approved: _____

Peter Monk, Ph.D.
Chairman of the Department of Mathematical Sciences

Approved: _____

Tom Apple, Ph.D.
Dean of the College of Arts and Sciences

Approved: _____

Daniel Rich, Ph.D.
Provost

ACKNOWLEDGMENTS

I wish to heavily thank Prof. Robert P. Gilbert for believing in me.

TABLE OF CONTENTS

LIST OF FIGURES

ABSTRACT

This thesis discusses the problem of the localization and identification of three-dimensional objects in a shallow water waveguide. This problem is an inverse problem. The observed data is the total wave field surrounding the body whose shape is to be reconstructed. The method involves using sound as an incident wave that will be scattered by the unknown body to create a scattered wave field. The problem is then solved by an inversion of the scattered wave-field. A least-squares matching of theoretical acoustic fields against the measured scattered field permits a reconstruction of the unknown object. A major portion of this project is the numerical results presented. Measurements involving the incident and scattered field are taken on a straight line on a plane above the unknown body, but below the top boundary of the waveguide. In the final chapter, we introduce an alternative route via the method of images. Our hope is that with this latter route, we can avoid some hardly scrutable mathematical tools we have used thus far.

Chapter 1

INTRODUCTION

The problem of identifying and reconstructing the image or shape of an unseen object has always been of great importance to several areas of science and technology. In the medical field for instance, the art and science of radiography deal with the problem of reconstructing medical images from measurements of the radiation around the body of a patient. One phenomenon common to most image reconstructions is that they are inverse problems; this means that the shape parameters of a model must be obtained by the manipulation of observed data.

1.1 Overview

This thesis disusses the problem of the localization and identification of three-dimensional objects in a shallow water waveguide. This problem is an inverse problem. The observed data is the total wave field surrounding the body whose shape is to be reconstructed. The method involves using sound as an incident wave that will be scattered by the unknown body to create a scattered wave field. The problem is is then solved by an inversion of the scattered wave-field. Measurements involving the incident and scattered field are taken on a straight line on a plane above the unknown body, but below the top boundary of the waveguide. In terms of position and shape parameters of the object, this inverse problem is nonlinear and fundamentally ill-posed. Furthermore, due to the multiple scattering of sound between the object and the top and bottom boundaries of the shallow water, the associated direct problem is way more complicated for a body in space.

We are going to use the intersecting canonical body approximation **ICBA** method. The **ICBA** method assumes that the amplitudes in the partial wave representation of the scattered field are nearly those of a canonical body. In an axially symmetric problem for example, the intersecting canonical body is usually a circular cylinder. This problem however is three-dimensional and for this reason, we are going to use a sphere as a canonical body. For more on the **ICBA** method, see the works by Gilbert, Scotti, Wirgin and Xu and Buchanan [9], [11], [12],[13],[1].

The assumption that the amplitudes in the partial wave representation of the scattered field are nearly those of a canonical body is true locally for each observation angle. Furthermore, the canonical body has the same local radius at this angle as that of the real body. It then makes sense to represent the shape of the body at each point, by its radius at a given angle. Thus, the reconstruction of the shape of the real body is done by the minimization of the the difference between the measured or simulated data and the estimation using a canonical body. This is done at each observation angle.

The procedure involved in the method we employ here, enables the reconstruction of the local radius of the body, for a given polar angle, by solving a single non-linear equation. See in this regard the seminal works by Scotti and Wirgin [21],[22],[23],[24], [25]. Another variant consists in finding this local radius by minimizing the L^2 cost functional of the difference between the simulated data and the estimation using a canonical body. Gilbert, Scotti, Wirgin and Xu [19], [20] extended these ideas to considering the **ICBA** in a waveguide. However, they used a cylinder as the canonical body in this three-dimensional problem. This led to inaccuracies on the upper-most and lower-most portions of the real body. The farfield patterns of acoustical waves scattered off an object in an acoustic waveguide with a pressure release surfaces and an elastic, or poroelastic, sea floors was investigated by integral equation methods in Gilbert et al [16], [17], [18], [4]. Gilbert, Lee and

Zeev [10] solved a similar problem using the same method. However, measurements involving the incident and scattered field were taken around the boundary of the body.

1.2 Applications

Among other application, this problem has important practical applications such as identification of mineral deposits, submarines, submerged navigational obstacles and wreckage, seamounts in harbors , *etc.*

1.3 Outline

In chapter two, we present a mathematical description and formulation of the problem. Chapter three discusses the inverse problems arising from the problem and chapter four illustrates some numerical results. In chapter five, we introduce an alternative route via the method of images. Our hope is that with this latter route, we can avoid some hardly scrutable mathematical tools we have used thus far.

Chapter 2

DESCRIPTION AND FORMULATION OF THE PROBLEM

In this chapter, we describe the problem under consideration and then present a precise mathematical formulation of the problem. The total acoustic wave field satisfies the Helmholts equation. For this reason, the focus here is to present the boundary conditions along with a series representation for the total acoustic pressure as a sum of the incident field and the scattered field.

2.1 Description of the problem

The essence of the problem is to identify the shape of submerged body in a sea of finite depth where the bottom of the sea is totally reflecting. In trying to solve this problem, we employ acoustic imaging using the **ICBA** method.

The ocean is restricted to lying between $z = h_2$ the surface and the bottom $z = -h_1$, thus, it occupies the space $\mathbf{R}^3_h = \mathbf{R}^2 \times [-h_1, h_2]$. See figure 2.1

2.2 Formulation of the problem

The submerged object occupies a domain Ω. Moreover, as we assume that the interrogating (incident) wave is monochromatic, we suppress the temporal component of the field $\exp(-i\omega t)$. Here ω is the angular frequency and t, the time.

The total acoustic pressure $u = u^i + u^s$, where u^i, u^s are the incident and scattered waves respectively, satisfies the Helmholtz equation:

$$(\Delta + \alpha^2)u = 0 \quad \text{in} \quad \mathbf{R}^3_h \backslash \bar{\Omega}, \tag{2.2.1}$$

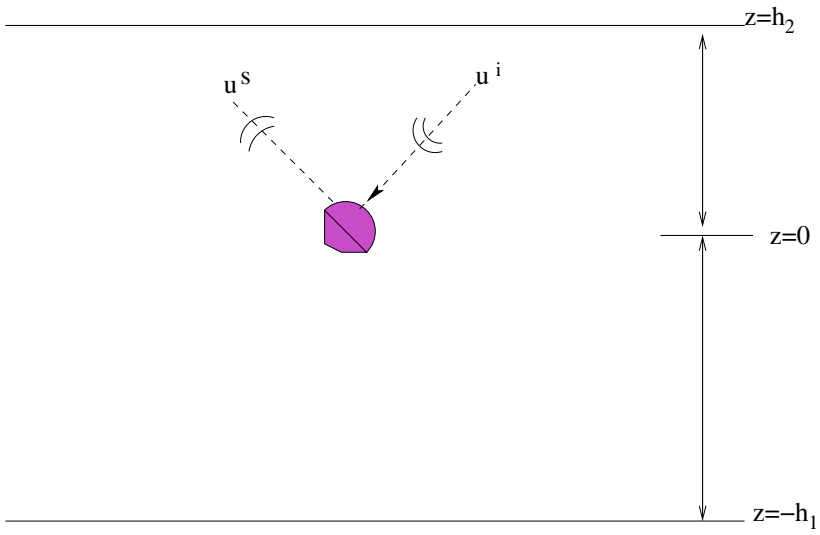

Figure 2.1: An object submerged in a shallow water of depth $h_1 + h_2$ units.

where $\alpha = \omega/c$, and c is the velocity of sound in the sea, which we assume is constant. We also assume the following boundary conditions:

$$\frac{\partial u(\rho, \theta, -h_1)}{\partial z} = 0, \quad u(\rho, \theta, h_2) = 0, \qquad u\big|_{\partial\Omega} = 0 \tag{2.2.2}$$

We shall consider an incident wave which satisfies the prescribed boundary conditions on the waveguide.

$$u^i = \sum_{j=1}^{J} e^{ix\sqrt{\alpha^2-\xi_j^2}} \sin \xi_j(z-h_2) = \sum_{j=1}^{J}\sum_{m=0}^{\infty} \epsilon_m i^m J_m(\sqrt{\alpha^2-\xi_j^2}\rho) \sin \xi_j(z-h_2)\cos m\theta, \tag{2.2.3}$$

where $\epsilon_m = 1$ for $m = 0$, $\epsilon_m = 2$ for $m > 0$, and $\xi_j = (j - \frac{1}{2})\pi/(h_1 + h_2)$, $j = 1, \ldots J$, where J is the integral part of $[\frac{1}{2} + \frac{\alpha(h_1+h_2)}{\pi}]$. The formulation of the problem makes use of the Rayleigh conjecture, which states that every point on an illuminated body radiates sound from that point as if the point lies on its tangent sphere. Consequently, it is necessary for us to solve the exterior Helmholtz problem for a sphere in a wave guide.

2.3 The total wave field

Outside any sphere enclosing the body the total wave field can be represented by

$$u(\rho,\theta,z) = u^i(\rho,\theta,z) + u^s(\rho,\theta,z) \tag{2.3.1}$$

with

$$\begin{aligned} u^s(\rho,\theta,z) = &\sum_{m=0}^{\infty} \int_0^{\infty} sJ_m(\rho s)\{a_m(s)e^{i\xi z} + b_m(s)e^{-i\xi z}\}ds \cos m\theta \\ &+ \sum_{n=0}^{\infty}\sum_{m=0}^{n} C_{nm} h_n^{(1)}(\alpha r) P_n^m(\cos\phi)\cos m\theta, \end{aligned} \tag{2.3.2}$$

where $\xi = \sqrt{\alpha^2 - s^2}$ if $s < \alpha$, $\xi = i\sqrt{s^2 - \alpha^2}$ if $s > \alpha$, and $h_n^{(1)}(\alpha r)$ is the spherical Bessel function of the third kind (defined by $h_n^{(1)}(s) = \sqrt{\pi/2s}H_{n+1/2}^{(1)}(s)$) and P_n^m is the associated Legendre function. Moreover, we use another version of Rayleigh's principle which states that the scattered solution can be analytically continued up to and including any part of a smooth part of the boundary of the scatterer. As a consequence, the inversion problem may be viewed as determining the Fourier coefficients in equation 2.3.2 . For how the analytical computation of these coefficients are done, see the appendix in Gilbert, Lee and Zeev [10].

Chapter 3

INVERSE PROBLEMS

In this chapter, we reformulate the problem as an inverse problem. We first consider a case where the submerged body is a sphere and then we proceed to any arbitrary three dimensional figure. The task boils down to approximating the radius of the body at a point as we take readings on the incident and scattered wave field at that point.

3.1 Inverse problem for a sphere

Assume the acoustic field is measured at the points (r_b, ϕ^q, θ^p), where the indices range over $q \in \{1, 2, \ldots, Q\}$ and $p \in \{1, 2, \ldots P\}$. The field at these points is given by $u^*(r_b, \phi^q, \theta^p)$, where r_b is a constant. The inverse problem is to determine $\eta^{qp} = \eta(\phi^q, \theta^p)$, for $q \in \{1, \ldots, Q\}$ and $p \in \{1, \ldots, P\}$ where we match off the data to its mathematical representation, namely

$$u^*(r_b, \phi^q, \theta^p) - \Bigg[u^i(r_b, \phi^q, \theta^p) + \sum_{m=0}^{M} \sum_{n=m}^{N} \Bigg\{ C_{nm}(\eta^{qp}) h_n^{(1)}(\alpha r_b)$$

$$-\frac{(n-m)!}{(n+m)!}(2n+1) j_n(\alpha r_b) \sum_{k=m}^{N} C_{km}(\eta^{qp}) I(k,n) \Bigg\} P_n^m(\cos\phi^q) \cos m\theta^p \Bigg] = 0, \quad (3.1.1)$$

The notation $C_{km}(\eta^{qp})$ indicates the dependence of C_{km} on η^{qp}. Note that $\eta(\phi, \theta)$ is not identically equal to the radius r_b because we have truncated the series for numerical purposes. $I(n, k)$ will be described in the next section.

3.2 Inverse problem for a three-dimensional object of arbitrary shape

We can extend the idea of the inverse problem for a sphere to arbitrary three-dimensional bodies provided we have already found the exterior solution for a sphere in a wave guide. Assume that the scatterer may be represented by a shape function $r(\phi,\theta)$ as $D = \{(r,\phi,\theta)|r = r(\phi,\theta), 0 \leq \phi \leq \pi, 0 \leq \theta \leq 2\pi\}$, where $r(\phi,\theta) \geq 0$. As before we first need to represent the solution to the direct problem. The analogy between the present problem and that of the sphere suggests the following approximation of the field.

$$u(r,\phi^q,\theta^p) = u^i(r,\phi^q,\theta^p) + \sum_{m=0}^{M}\sum_{n=m}^{N}\big\{C_{nm}(r(\phi^q,\theta^p))h_n^{(1)}(\alpha r)$$

$$-\beta_{nm}j_n(\alpha r)\sum_{k=m}^{N}C_{km}(r(\phi^q,\theta^p))I(k,n)\big\}P_n^m(\cos\phi^q)\cos m\theta^p, \tag{3.2.1}$$

where $\beta_{nm} = (2n+1)(n-m)!/(n+m)!$ and the coefficients C_{nm} have been found from the solution to the exterior problem mentioned above. In the Appendix of Gilbert, Lee and Zeev [10], the coefficients $C_{nm}(r(\phi^q,\theta^p))$ were found to be given by

$$C_{nm}(r^{qp})h_n^{(1)}(\alpha r^{qp}) + \beta_{nm}j_n(\alpha r^{qp})\Bigg[-\sum_{k=m}^{N}C_{km}(r^{qp})I(k,n)$$

$$+\epsilon_m i^m\sum_{j=1}^{J}P_n^m(\tfrac{\xi_j}{\alpha})\Im(i^{n-m}e^{-i\xi_j h_2})\Bigg] = 0, \quad (n = m, m+1, \cdots, N) \tag{3.2.2}$$

where $r^{qp} = r(\phi^q,\theta^p)$, ξ_j is defined as in section 2.2 and j_n is the spherical Bessel function of the first kind defined by $j_n(\zeta) = \sqrt{\frac{\pi}{2\zeta}}J_{n+\frac{1}{2}}(\zeta)$.

$I(n,k)$ is defined by the following contour integral

$$I(n,k) = i^{n-k} \int_0^\infty \frac{s P_k^m(\frac{\xi}{\alpha}) P_n^m(\frac{\xi}{\alpha})}{2\alpha\xi \cos\xi(h_1+h_2)} \Big[e^{i\xi(h_1+h_2)}\{1+(-1)^{k+n}\}$$

$$-(-1)^{k-m} e^{i\xi(h_1-h_2)} + (-1)^{n-m} e^{-i\xi(h_1-h_2)} \Big] ds, \tag{3.2.3}$$

where the path of integration is indented below all poles on the real axis.

We formulate the inverse problem as determining the discrete shape function r^{qp} on the index set $q \in \{1,\ldots,Q\}$ and $p \in \{1,\ldots,P\}$ such that

$$u^*(r_b,\phi^q,\theta^p) - \Big[u^i(r_b,\phi^q,\theta^p) + \sum_{m=0}^{M} \sum_{n=m}^{N} \{C_{nm}(r^{qp}) h_n^{(1)}(\alpha r_b)$$

$$-\beta_{nm} j_n(\alpha r_b) \sum_{k=m}^{N} C_{km}(r^{qp}) I(k,n)\} P_n^m(\cos\phi^q)\cos m\theta^p \Big] = 0. \tag{3.2.4}$$

Here $u^*(r_b,\phi^q,\theta^p)$ are given data and the sum represents the total field expression for a sphere with radius r^{qp}.

Chapter 4

NUMERICAL EXPERIMENTS

We obtained some numerical results using the following parameters. $h_1 = 2$ m, $h_2 = 3$ m, $r_b = 2.5$m, $\alpha r_b = 1.8$, $J = 1$, $\xi_1 r_b = 0.7$, $N = 10$ and $M = 5$. The first computation is the numerical simulations of 'measured' data for a sphere of radius r_b. This was conducted for the incident wave using equations 3.2.1 and 3.2.2. The second step is to take M and N equal to 7 and solve equation 3.2.4 in a least square sense for each $r(\phi^q, \theta^p)$.

Figure 4.1 shows the pictures of an ellipsoid and its reconstruction. The equation of the original ellipsoid is

$$\frac{\rho^2}{1.5^2} + \frac{z^2}{1^2} = 1.$$

Figure 4.2 shows the pictures of an ellipsoid and its reconstructed image. The original torus is described parametrically as

$$z = (c + a\cos v)\cos u \quad y = (c + a\cos v)\sin u \quad x = a\sin v$$

with c=1 and a=1/2.

The last reconstruction is that of an astroid-like three dimensional body shown in figure 4.3. The original figure is described parametrically as

$$x = \cos^3 u \cos^3 v \quad y = \sin^3 u \cos^3 v \quad z = \sin^3 v$$

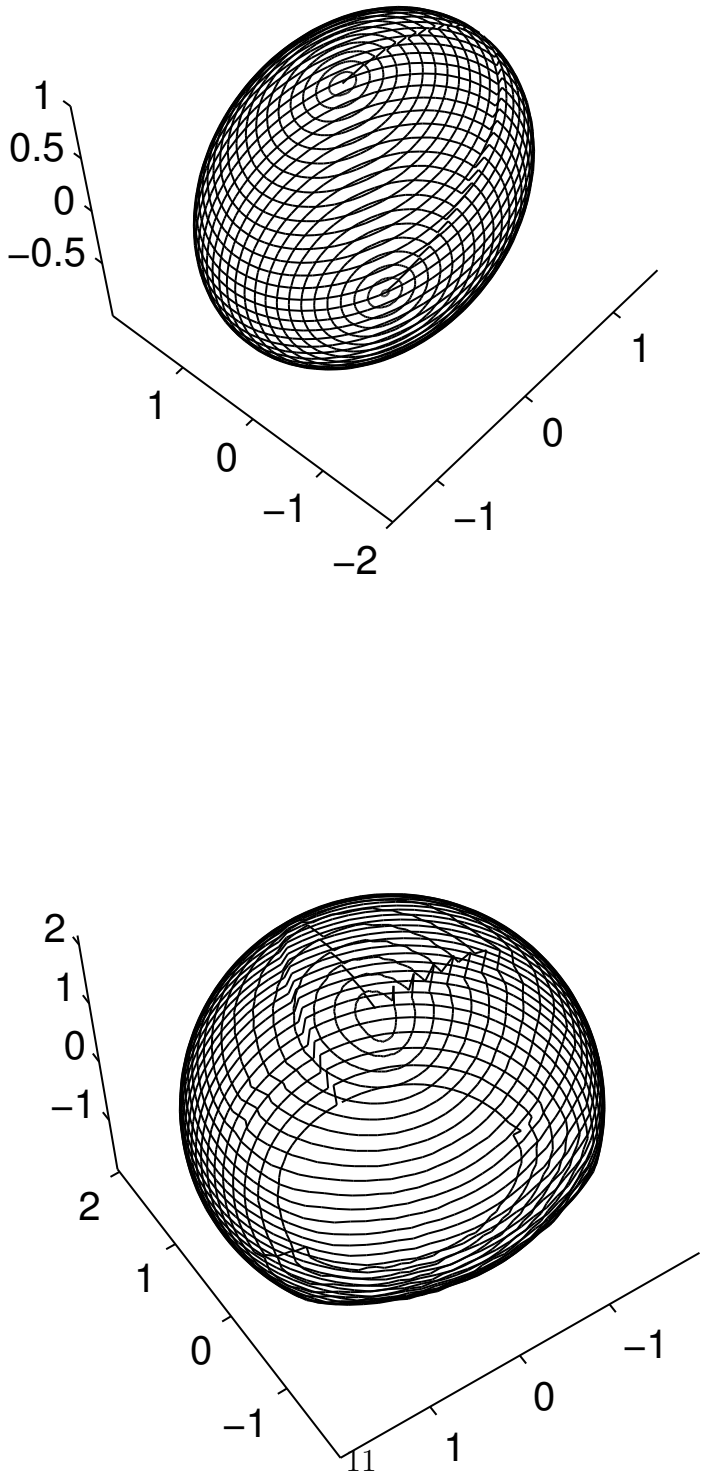

Figure 4.1: Original ellipsoid (top); reconstructed ellipsoid (bottom)

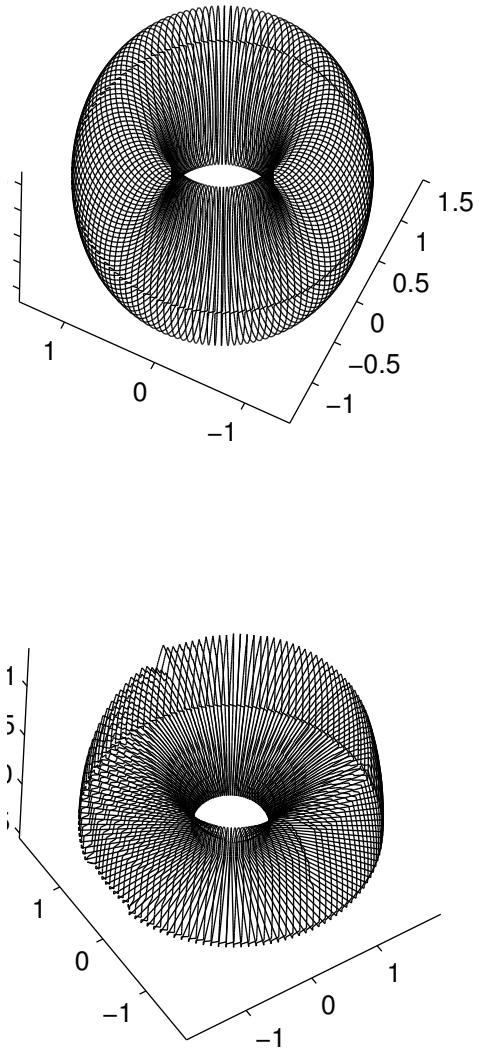

Figure 4.2: Original torus (top); reconstructed torus (bottom)

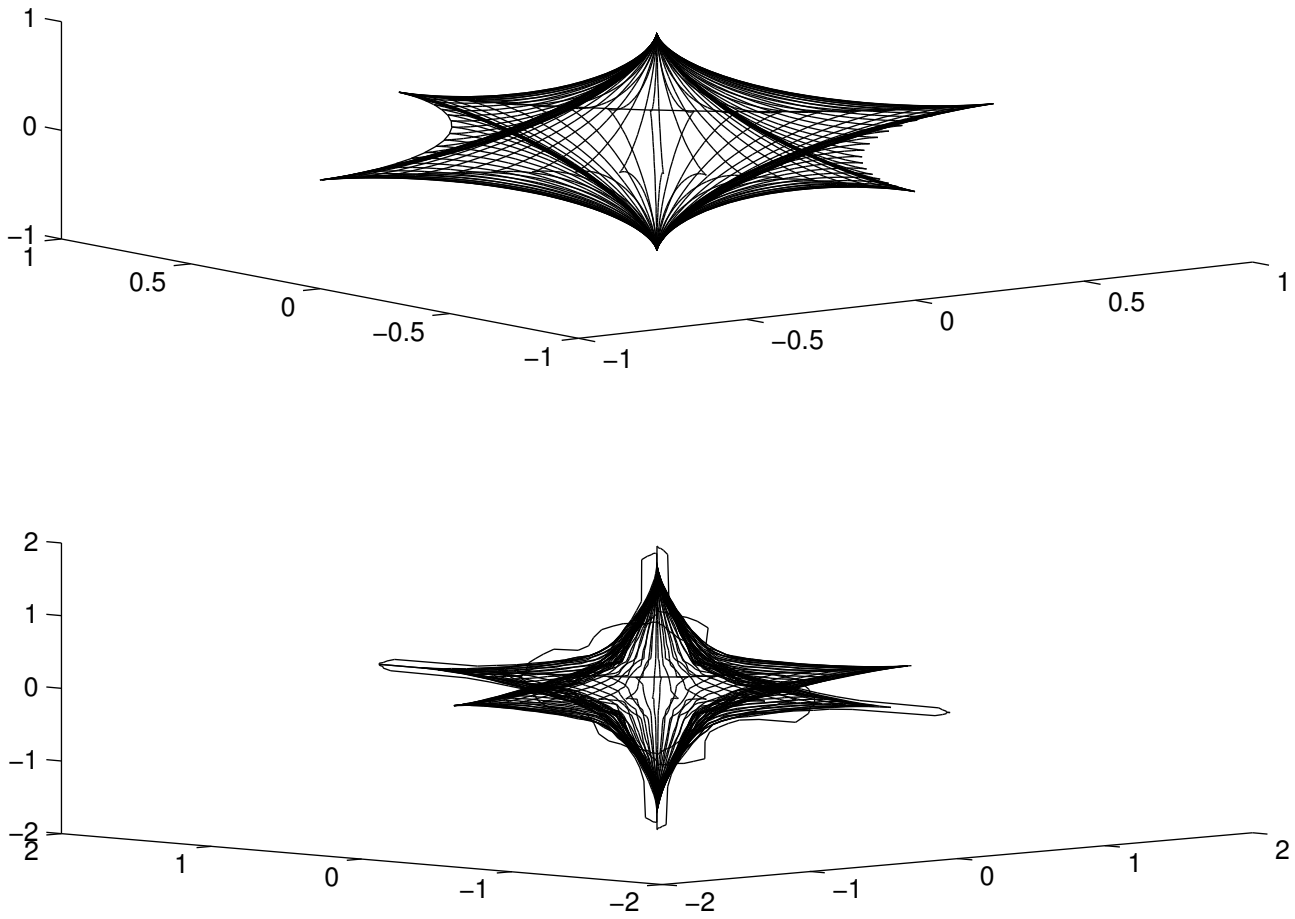

Figure 4.3: Original astroid(top); reconstructed astroid (bottom)

Chapter 5

AN INTRODUCTION TO AN ALTERNATE APPROACH VIA THE METHOD OF IMAGES

It is obvious that the mathematical tools used in this project are somewhat complicated in nature, due to the special functions involved. This gives rise expensive and possibly inefficient computations. For this reason, one begins to wonder if there is another approach to this shape reconstruction problem that will avoid special functions.

We now turn to a simpler problem, which is more amenable to the method of images. In the case of electrostatics, Laplace's equation plays an important role.

5.1 Solution to the Laplace's equation outside a sphere

Here, we are going to focus on the solution to the Laplace's equation outside a sphere. To this end, we make some introductory remarks about electrostatics. The electric field is related to the charge density by

$$\nabla \cdot E = \frac{\rho}{\epsilon_0} \tag{5.1.1}$$

where E is the electric field, ρ, the charge density and ϵ_0, the permitivity.

The electric field is related to the electric potential, V, by the gradient relationship

$$E = -\nabla V \quad . \tag{5.1.2}$$

Thus the electric potential is related to the charge density by the Poisson's equation

$$\nabla \cdot \nabla V = \Delta V = -\frac{\rho}{\epsilon_0} \tag{5.1.3}$$

In a charge-free region of space, $\rho = 0$ and 5.1.3 becomes the Laplace's equation

$$\Delta V = 0 \tag{5.1.4}$$

Since we are dealing with a sphere, the solution to 5.1.4 will be easy to determine in spherical coordinates. In spherical coordinates, 5.1.3 becomes

$$\Delta V = \frac{\partial^2 V}{\partial r^2} + \frac{1}{r^2}\frac{\partial^2 V}{\partial \theta^2} + \frac{1}{r^2 \sin^2\theta}\frac{\partial^2 V}{\partial \phi^2} + \frac{2}{r}\frac{\partial V}{\partial r} + \frac{\cot\theta}{r^2}\frac{\partial v}{\partial \theta} = \frac{-\rho}{\epsilon_0} \tag{5.1.5}$$

However, to take advantage of the full spherical symmetry, the derivatives with respect to θ and ϕ will all be set equal to zero. 5.1.5 will therefore become

$$\frac{\partial^2 V}{\partial r^2} + \frac{2}{r}\frac{\partial V}{\partial r} = \frac{-\rho}{\epsilon_0} \tag{5.1.6}$$

Outside the sphere, we make use of equation 5.1.4 which, in spherical coordinates, has the form

$$\frac{\partial^2 V}{\partial r^2} + \frac{2}{r}\frac{\partial V}{\partial r} = 0 \tag{5.1.7}$$

Solutions to equation 5.1.7 are thus of the form

$$V = \frac{a}{r} + b \tag{5.1.8}$$

If we choose to assign the zero potential to infinity i.e $V \to 0$ and $r \to \infty$, we obtain that $b = 0$. We normalize this solution by setting $a = \frac{q}{4\pi\epsilon_0}$. Then the solution to Laplace's equation exterior to the sphere is

$$V = \frac{q}{4\pi\epsilon_0 r} \tag{5.1.9}$$

where q is a point charge in a free space outside the sphere and r is its distance from a point of reference on the sphere.

5.2 Reflecting a source through a sphere

We consider spherical equipotential surfaces. To this end, consider a sphere of radius a and center O. Assume that a point charge q_1 is placed at a distance r_1 from P, a point of reference on the sphere. This charge causes the sphere to lose its equipotentiality. To preserve the equipotentiality of the sphere, q_1 needs to have an image inside the sphere. We want to determine q_2, the image of q_1 inside the sphere. Let r_2 be the distance of q_2 from P as shown on figure 5.1. Let the distance between O and q_1 be b and the distance between O and q_1, r. We want to obtain

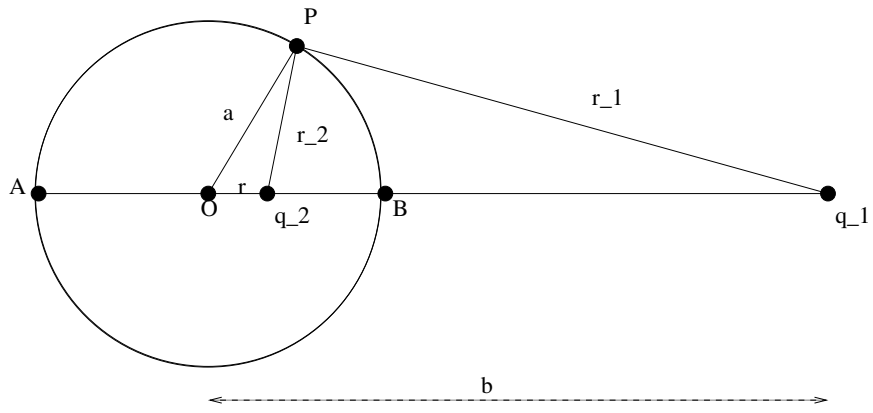

Figure 5.1: Determining q_2

an expression for q_2 and r in terms of q_1, a and b. To preserve the total potential of the sphere, the potential resulting from q_1 must be equal to that resulting from q_2. For this reason, if we consider the point A, on the sphere in 5.1, we have that

$$\frac{q_1}{4\pi\epsilon_0(b+a)} + \frac{q_2}{4\pi\epsilon_0(r+a)} = 0 \tag{5.2.1}$$

If we now consider the point B, we get

$$\frac{q_1}{4\pi\epsilon_0(b-a)} + \frac{q_2}{4\pi\epsilon_0(a-r)} = 0 \tag{5.2.2}$$

From 5.2.1 and 5.2.2 we obtain

$$q_1(r+a) + q_2(b+a) = 0$$

$$q_1(a-r)+q_2(b-a)=0$$

Adding these two relations eliminates r and gives $2q_1a+2q_2b=0$. This implies that

$$q_2=-q_1\frac{a}{b} \tag{5.2.3}$$

If we subtract the two equations, we obtain $2q_1r+2q_2a=0$, which gives that $r=-a\frac{q_2}{q_1}$. By making use of 5.2.3, we end up with an expression for r in terms of a and b.

$$r=\frac{a^2}{b} \tag{5.2.4}$$

5.3 Equipotentiality of a system of a sphere and one plane

Consider a point charge q_0 at the center of a sphere and a plane L placed h units from the sphere as shown in figure 5.2.

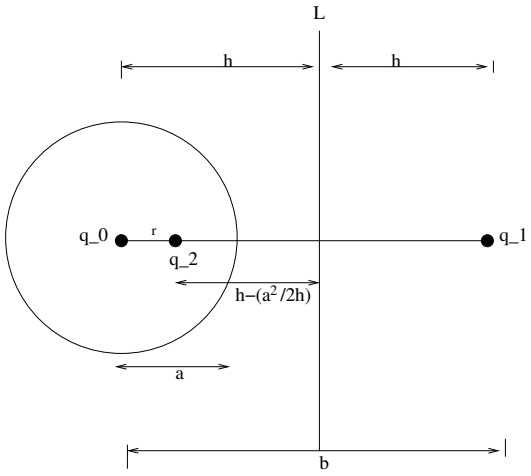

Figure 5.2: Geometry of the image of a charge (1)

Let us make a little adjustment to figure 5.2. Instead of having the plane by the side, we have it h units above the center of the sphere.

Before introducing the plane to the system, we assume that the sphere is of a constant non-zero potential and that the plane is of zero potential. Consider the

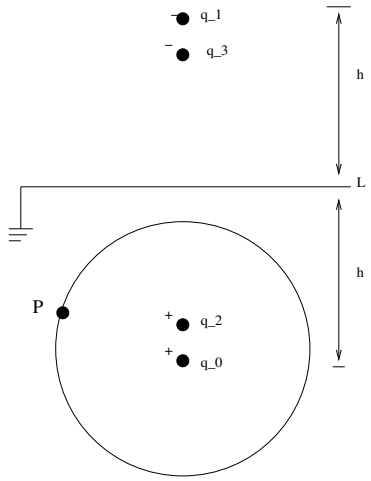

Figure 5.3: Geometry of the image of a charge (2)

charge q_0 at the center of the circle. Once the plane is introduced into the system, q_0 is going to induce a potential to it. For the plane to maintain its zero potentiality, we need an image charge equal but opposite to q_0 to equalize the potential due to q_0. If we let q_1 be the image q_0 on the other side of the sphere keeping it $2h$ units away from q_0, we notice that, although the plane is now an equipotential body, the system is no longer equipotential since, the sphere just loses its equipotentiality. We now take a look the image q_2 of q_1. From our discussion in the preceeding section, we gather that q_2 is $h - \frac{a^2}{2h}$ units away from the plane L and $q_2 = -\frac{a}{2h}q_1 = \frac{a}{2h}q_0$. By adding q_2, the plane loses its equipotentiality. For this reason we add q_3 above the plane and then q_4 and we continue this way until we get the system to be equipotential. q_3 is equal but opposite to q_2 implying $q_3 = \frac{a}{2h}q_0$ and $q_4 = \frac{a}{(2h)^2}q_0$. We need to mention that these charges all lie on a imaginary straight vertical line as shown in figure 5.3. If we assume that the center of the sphere is at the origin, we can summarise all the charges $\{q_k\}$ and their positions $\{p_k\}$ on the cartesian coordinate system as follows:

$$q_0 \qquad p_0 = (0, 0, -h)$$

$$q_2 = \frac{a}{2h}q_0 \qquad p_2 = (0,0,-h+\frac{a^2}{2h})$$
$$q_4 = \frac{a^2}{(2h)^2}q_0 \qquad p_4 = (0,0,-h+\frac{2a^2}{2h})$$
$$\vdots$$
$$q_{2k} = \frac{a}{2h}^{k} q_0 \qquad p_{2k} = (0,0,-h+\frac{ka^2}{2h})$$

We also obtain the following:

$$q_1 = -q_0 \qquad p_1 = (0,0,h)$$
$$q_3 = -\frac{a}{2h}q_0 \qquad p_3 = (0,0,h-\frac{a^2}{2h})$$
$$q_5 = -\frac{a^2}{(2h)^2}q_0 \qquad p_5 = (0,0,h-\frac{2a^2}{2h})$$
$$\vdots$$
$$q_{2k+1} = -\frac{a}{2h}^{k} q_0 \qquad p_{2k+1} = (0,0,h-\frac{ka^2}{2h})$$

If we now consider the arbitrary point $P(x_p, y_p, z_p)$, as shown in figures 5.1, 5.2 and 5.3, the potential at this point is thus

$$V_p = \frac{1}{4\pi\epsilon_0}\sum_{k=0}^{k=\infty}(\frac{q_{2k}}{r_{2k}} + \frac{q_{2k+1}}{r_{2k+1}}) \tag{5.3.1}$$

where

$$r_{2k} = \sqrt{x_p^2 + y_p^2 + (z_p + h - \frac{ka^2}{2h})}^{2} \tag{5.3.2}$$

$$r_{2k+1} = \sqrt{x_p^2 + y_p^2 + (z_p - h + \frac{ka^2}{2h})}^{2} \tag{5.3.3}$$

5.4 Equipotentiality of a system of a sphere between two parallel planes

We now consider the case where the sphere centered at the origin is placed between two planes, one $z = h$ and the other $z = -l$. We need an expression for the total potential at a point. However, we first describe the scheme for calculating the charges for the solution to the Laplace's equation.

5.4.1 Calculating the series of charges to create equipotentiality

Creating equipotentiality of the system of a sphere and two paralell planes is little more complicated than that of one plane. We mark with ($'$) all the charges either located below the lower plane or reflected by charges below the lower plane. The best way to describe this scheme of imaging involved is to label the stages involved.

Stage zero:At this stage we consider a point charge q_0 located at the center of the sphere.

Stage one: q_0 gives rise to images q_1 and q_1' above the upper plane and below the lower plane respectively.

Stage two: q_1 and q_1' both yield their respective images q_2 and q_2' inside the sphere.

Stage three: q_2 and q_2' respectively reflect q_{3_1} and q_{3_2} above the upper planes and q_{3_1}' and q_{3_2}' below the lower plane

Stage four: q_{3_1} and q_{3_2} reflects q_{4_1} and q_{4_2} inside the sphere and q_{3_1} and q_{3_2} reflect q_{4_1}' and q_{4_2}' inside the sphers.

This process continues infinitely. This scheme is represented diagramatically in 5.4, 5.5, 5.6, 5.7, 5.8 The book-keeping involved in this scheme is tedious. However it possible to note the following pattern:

For $n = 1, 2, 3, \ldots$

Stage 2n: equal number of charges are reflected into the sphere from above the upper plane and below the lower plane. The total number of charges reflected into the sphere is equal to the number of image charges produced in the previous stage.

Stage 2n-1: equal number of charges are reflected above the upper plane and below the lower plane from inside the sphere. The total number of charges reflected into the sphere is equal to double the number of image charges produced in the previous stage.

We also have that all charges outside the sphere are negative and those inside

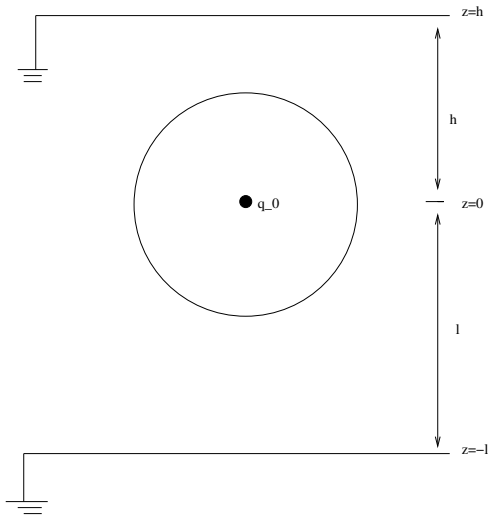

Figure 5.4: Images of charges in a sphere and two planes system. stage 0

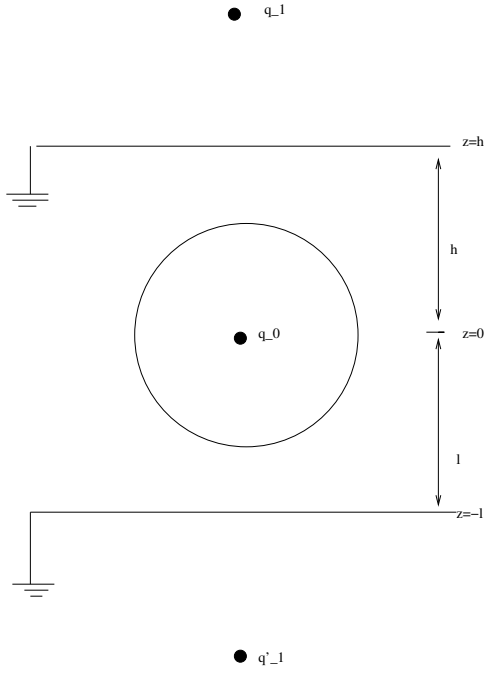

Figure 5.5: Images of charges in a sphere and two planes system. stage 1

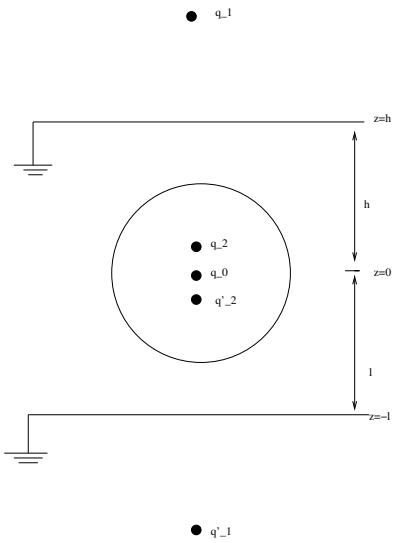

Figure 5.6: Images of charges in a sphere and two planes system. stage 2

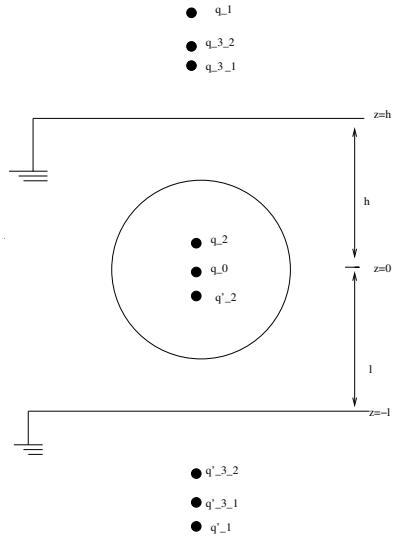

Figure 5.7: Images of charges in a sphere and two planes system. stage 3

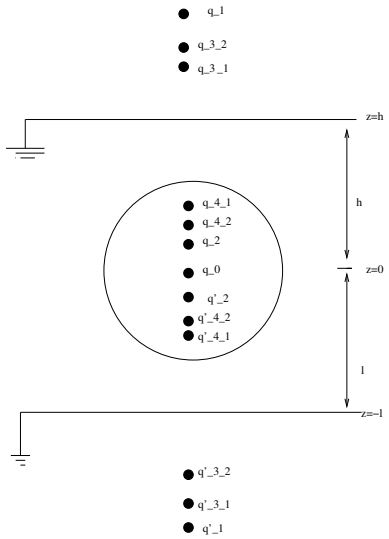

Figure 5.8: Images of charges in a sphere and two planes system. stage 4

the sphere are positive.

The formula for the total potential similar to that in 5.3.1 is far from succinct. We avoid dealing with this by writing a computer program that computes of charges and their positions at each stage, computes the total potential and plots the level curve for $V = c$. Formulas 5.2.3 and 5.2.4 are still used to compute the magnitude and position of an image charge.

5.4.2 Some numerical investigations

We now perform some numerical experiment to investigate the set of points at which the system has a constant potential. With y set to zero, figure 5.9 gives the level curves for $4\pi\epsilon_0 V = c$ where V is the function of x and z as described in 5.3.1 with the series truncated at $k = 1000$. For this computation, $q_0 = 1$, $a = 1$, $\epsilon_0 = 1$, $h = 2$ and $l = 2.5$. It can be observed that at the level, $c = 1$, we obtain a circular figure quite close to a circle of radius $a = 1$ and at $c = 0$, we obtain lines that approximate the upper and lower planes.

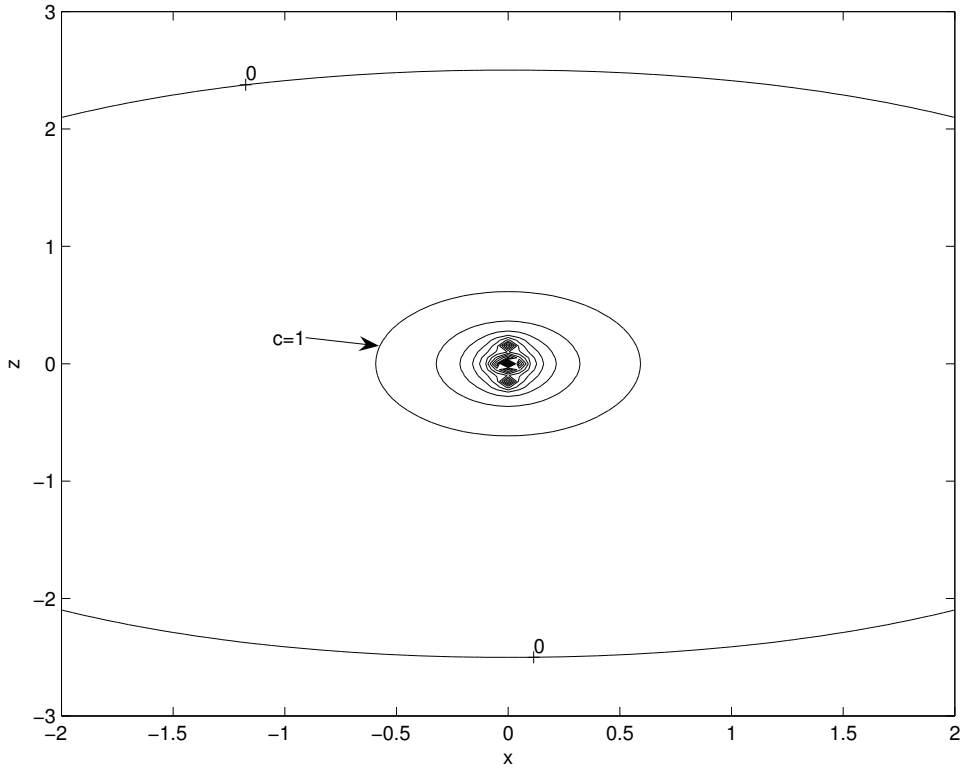

Figure 5.9: Level curves for $V = c$

5.5 A possible inverse problem

The next direction of this work would be to try to extend this idea of images to the Helmholtz equation in a waveguide.

BIBLIOGRAPHY

[1] Buchanan, J.L., Gilbert, R. P., Wirgin, A., and Xu,Y.S., 2000, Identification, by the intersecting canonical domain method, of the size, shape and depth of a soft body of revolution located within an acoustic wave guide, *Inverse Problems* **16** 1709-1726

[2] D. Colton and P. Monk. A novel method of solving the inverse scattering problem for time-harmonic acoustic waves in the resonance region. *SIAM J. Appl. Math,* 45:1039-1053, 1985.

[3] D. Colton and P. Monk. A novel method of solving the inverse scattering problem for time-harmonic acoustic waves in the resonance region II: *SIAM J. Appl. Math,* 46:506-523, 1986.

[4] Buchanan, J.L., Gilbert, R. P., Wirgin, A., and Xu,Y.S., 2004, Marine Acoustics: Direct and inverse Problems, SIAM, Philadelphia.

[5] Bucker, H.P. 1976 Use of calculated sound fields and matched field-detection to locate sound sources in shallow water. *J.Acoust.Soc. Am.***59** 368-73

[6] D. Colton, J. Coyle, and P. Monk. Recent developments in inverse acoustic scattering theory.*SIAM Review,* 42:369-414, 2000.

[7] Smythe, W. R. 1968, Static and Dynamic Electricity, Third Edition, McGraw-Hill. 121-141

[8] Cook, J.C. 1962, On potential problems involving spheroids inside a cylinder. Z. angew. Math. Mech. **42** 305-316

[9] Buchanan, J. L. and Gilbert, R. P. and Wirgin, A., 1998, Finding an inclusion in a shallow ocean using a canonical domain method, in PROCEEDINGS OF THE FOURTH EUROPEAN CONFERENCE ON UNDERWATER ACOUSTICS,eds. A. Alippi and G.B. Canneli, CNR-IDAC, Rome, 389-394

[10] Gilbert, R. P., Lee, D. S., Zeev, N., 2005, Classification of objects in an acoustic waveguide by inversion of the farfield data *Computational Acoustics*

[11] Buchanan, J.L., Gilbert, R. P., Wirgin, A., and Xu,Y.S., 1999, The unidentified object problem in a shallow ocean with a fluid-like sediment layer overlying a rigid sea bed, *Applicable Analysis* **73** 5-17

[12] Buchanan, J. L. and Gilbert, R. P. and Wirgin, A., 1999 Finding an inclusion in a shallow ocean using the ICBA method, *Applicable Analysis*, **71**, 347-378

[13] Buchanan, J. L. and Gilbert, R. P. and Wirgin, A., 1999, Implementation of the ICBA method for solids of revolution, *Problemi Atuali dell'Analisi e della Fisica Matematica*, Aracne, Rome

[14] Erdélyi, A. 1937 Zur Theorie der Kugelwellen *Physica IV* no 2 107-120

[15] Gilbert, R.P. and Xu, Y., 1996, The seamount problem, 140 in *SIAM Special Issue on the Occasion of Prof. I.Stakgold's 70th birthday, Nonlinear Problems in Applied Mathematics,* Angell T. et al. Ed., SIAM, Philadelphia

[16] Gilbert, R.P. and Lin, Z. 1997 Scattering in a shallow ocean with an elastic seabed *Comput.Acoust.*, **5** 403-31

[17] Gilbert, R. P. and Lin Z. 1998 The Fundamental singularity in a shallow ocean with an elastic seabed. *Applicable Analysis*, **68**, 87-99

[18] Gilbert R. P. and Lin Z. 1997 Acoustic field in a shallow stratified ocean with a poro-elastic seabed. *ZAMM* , **77**, 677-688

[19] Gilbert, R.P. and Scotti, T. and Wirgin, A. and Xu, Y. 1998 The unidentified object problem in a shallow ocean, *J. Acoustical Soc. Am.* **103**, 1-8

[20] Gilbert, R.P. and Scotti, T. and Wirgin, A. and Xu, Y. 1997 Identification of a 3D object in a shallow sea from scattered sound, *C.R. Acad. Sci. Paris IIb*, **325**, 383-389

[21] , Scotti, T. and Wirgin, A. 1995 Location and shape reconstruction of a soft body by means of canonical solutions and measured scattered sound fields, *C. R. Acad. Sci. Paris II b*, **330**, 641-646

[22] , Scotti, T. and Wirgin, A. 1995 Shape reconstruction using diffracted waves and canonical solutions, *Inverse Problems*, **11**, 1097-1111

[23] Scotti, T. and Wirgin, A. 1996 Shape construction of an impenetrable scattering body via the Rayleigh hypothesis, *Inverse Problems*, **12**, 1027-1055

[24] Scotti, T. and Wirgin, A. 1997 Shape construction of a penetrable homogeneous 3D scattering body via the ICBA, in Inverse Problems of Wave Propagation and Diffraction, ed. G. Chavent and P. Sabatier, Springer, Berlin, 367-372

[25] Scotti, T. and Wirgin, A. 1998 Location and shape reconstruction of an impenetrable 3D body by matching measurements of scattered sound to a canonical body field representation, in Inverse Problems in Engineering : Theory and Practice, ASME International, New York, 29-36

[26] Watson, G.N. *A Treatise on the theory of Bessel functions*, p.370, 2nd ed. Cambridge. Cambridge Univ.Press 1962